Biophysical Journal
Article

Biophysical Society

Non-equilibrium Membrane Homeostasis in Expanding Cellular Domains

P. Rowghanian[1] and O. Campàs[1,*]
[1]Department of Mechanical Engineering and California NanoSystems Institute, University of California, Santa Barbara, Santa Barbara, California

ABSTRACT Many cell behaviors involve cell-shape transformations that impose considerable changes in the cell's surface area, requiring a constant adaptation of the cell's plasma membrane area to prevent cell lysis. Here, we theoretically describe the interplay between the plasma membrane dynamics and a physically connected cell cortex or wall, accounting for spatial variations in membrane recycling and tension. In-plane membrane net flows result naturally from these dynamics and, in the presence of an expanding cell cortex or wall, regions of converging or diverging flow patterns emerge. These flow patterns can potentially explain the spatial localization/segregation of membrane proteins in processes such as cell polarization. We also identify the relevant parameters that control membrane homeostasis and derive the range of parameters for which homeostatic states exist.

INTRODUCTION

Both animal cells and walled cells, such as those of plants, bacteria or fungi, undergo cell shape transformations that involve large changes in cell surface area (1–3). Although the mechanics of cell shape changes is essentially governed by the actomyosin cytoskeleton in animal cells (4) and the cell wall in walled cells (1), the cell's plasma membrane has to adapt to the imposed surface area changes that occur during shape transformations to avoid rupture of the plasma membrane and cell death (2,3,5–7). These events result in membrane tension variations that affect many cellular processes (8,9).

Several mechanisms of plasma membrane area adaptation act at different timescales and are able to buffer membrane variations by different amounts (5–7). In animal cells, structures such as caveolae act as membrane reservoirs and help buffer fast (<1 min), albeit small (∼1%), changes in area (6,10). Other mechanisms, such as blebbing (11,12) or membrane ruffling (6), allow animal cells to buffer relatively rapid (∼1 min) and intermediate changes in surface area (∼50%) imposed by cytoskeletal mechanics (13,14). All these mechanisms, which have been previously studied theoretically (11,15,16) and experimentally (6), rely on a plasma membrane with different membrane reservoirs but fixed total area. However, large changes in cell area require either localized or global membrane recycling through a combination of endo- and exocytosis (1,2). Unlike animal cells, walled cells rely almost completely on endo- and exocytosis to adapt plasma membrane surface area, as their internal turgor pressure prevents membrane reservoirs in the forms of membrane ruffles, blebs, or caveolae (1,3). Membrane recycling is thus crucial for plasma membrane area adaptation to large variations in cell surface area occurring at timescales characteristic of cell shape changes, especially in processes such as axonal growth (animal cells (2)) and tip growth (walled cells (1)). However, it remains unclear how membrane homeostasis is achieved in these conditions, in which expanding domains of the cell surface impose large plasma membrane variations during cell morphogenesis.

Beyond area regulation, plasma membrane recycling also results in exo- and endocytosis of specific transmembrane proteins that affect the structural and mechanical states of the actomyosin cortex (17) and/or the cell wall (18), thereby indirectly affecting the mechanical events that control cell shape changes. Additionally, both membrane recycling and the resulting plasma membrane dynamics may affect the distribution and movements of transmembrane proteins, which could be essential for various cellular processes, such as cell polarization (19,20). The effect of membrane dynamics on all these events remains largely unknown.

Given that membrane area regulation through exo- and endocytosis is critical for walled cells, we develop a theoretical description of the dynamics of an actively recycled plasma membrane subject to area changes imposed by the

Submitted March 31, 2017, and accepted for publication June 2, 2017.
*Correspondence: campas@engineering.ucsb.edu
Editor: Cecile Sykes.
http://dx.doi.org/10.1016/j.bpj.2017.06.001

expansion of the neighboring cell wall (Fig. 1), which bears the mechanical load and controls the cell area expansion. We find that in the absence of cell wall expansion, localized membrane recycling through exo- and endocytosis leads to diverging (outward) membrane flows from the region where recycling is most active. In the presence of a localized cell wall expansion, the competing effects of localized membrane recycling and expansion lead to the appearance of a finite-size region with converging membrane flows inside it and diverging flows outside of it. If localized membrane recycling is supplemented with global membrane recycling, new membrane flow patterns emerge. The predicted in-plane plasma membrane flow patterns with converging flows provide a natural mechanism to sustain cell polarization, as membrane-localized proteins can be accumulated in regions with converging flows. Finally, we establish the parameters that control the dynamical regimes of the system and show that membrane recycling cannot always adapt and follow cell expansion. These results highlight the relevance of the interplay between wall expansion and active membrane recycling to understanding the dynamics of the plasma membrane and of membrane-localized proteins.

METHODS

Theoretical description

For the sake of simplicity, we consider an infinite one-dimensional (1D) cell membrane with mass density $\rho(x,t)$ that represents a local measure of the membrane excess area. Membrane material can be added and removed at each point through exocytosis and endocytosis at rates k_X and k_D, respectively. In general, the membrane is characterized by a tension profile, $\sigma(x,t)$, and can display a net in-plane flow with velocity profile $v(x,t)$, which is opposed by friction with the surrounding fluid and also by friction arising from transmembrane proteins connected to the neighboring wall (9,21,22) (Fig. 1). Given that the system is overdamped, local force balance on the membrane reads (22)

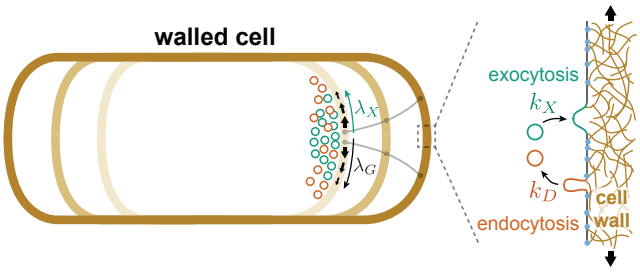

FIGURE 1 Sketch depicting a growing walled cell (e.g., fission yeast; cell wall is depicted darker for increasing time points). As the cell grows, the wall expands (*black arrows*) in some regions (*gray dots* and *lines* show the relative expansion of the cell wall upon cell growth). In these expanding regions, exo- and endo-cytosis must be able to provide enough new membrane to follow the local cell surface expansion imposed by the cell wall (endocytic vesicles, *red*; exocytic vesicles, *green*). Cell expansion and exocytosis are localized by the cell to regions of sizes λ_G and λ_X from the tip, respectively. Transmembrane proteins (*blue dots*) connect the plasma membrane (*gray*) to the cell wall. To see this figure in color, go online.

$$\partial_x \sigma = \xi v + \xi_2 (v - u), \tag{1}$$

where ξ and ξ_2 are the friction coefficients of the membrane with the surrounding fluid and with the neighboring wall, respectively (22). The velocity profile, $u(x,t)$, corresponds to the local velocity of the neighboring wall and is considered herein an input field as described below. Membrane mass conservation in the presence of recycling reads

$$\partial_t \rho + \partial_x (\rho v) = k_X \rho_X^0 - k_D \rho, \tag{2}$$

where ρ_X^0 is the average membrane density of exocytic vesicles. In what follows, we focus on the case of uniform plasma membrane density, ρ_0, which is characteristic of walled cells, where little to no excess area can be stored because of turgor pressure. We have checked that our results do not qualitatively change if the membrane density is non-uniform (up to variations of $\sim$30%, i.e., $1 < \rho/\rho_0 \lesssim 1.3$). Membrane homeostasis, characterized by the steady-state membrane dynamics, is obtained from Eqs. 1 and 2. Specifically, the steady-state tension profile is given by

$$\frac{1}{\xi + \xi_2} \frac{d^2\sigma}{dx^2} = \frac{\rho_X^0}{\rho_0} k_X - k_D - \frac{\xi_2}{\xi + \xi_2} \mathcal{G}(x), \tag{3}$$

where $\mathcal{G}(x) = \partial_x u$ is the local area expansion rate, or strain rate, of the wall. When the friction from the connection between the membrane and wall is much stronger than friction with the surrounding medium ($\xi \ll \xi_2$), Eq. 3 describes a membrane in an expanding geometry with local areal expansion rate $\mathcal{G}(x)$.

The functional form of $\mathcal{G}(x)$, which we consider an input in our description, can be obtained experimentally (23,24) or by solving the mass and momentum conservation equations for the cell wall (25), as it is the wall (not the membrane) that mechanically sustains the internal cell's pressure and sets its local expansion rate. Given that many morphogenesis problems of walled cells involve a localized wall expansion (e.g., tip growth), we impose a localized cell wall expansion rate $\mathcal{G}(x) = (g/\sqrt{2\pi})\exp(-x^2/(2\lambda_G^2))$ (with g and λ_G being the characteristic magnitude and lengthscale, respectively, of the wall expansion) and study how such an expansion profile affects the plasma membrane dynamics. More complex expansion profiles can be described as combinations of local expansions by letting $\lambda_G \to 0$ and considering $\mathcal{G}(x)$ as the Green's function of the dynamics.

To solve Eq. 3, it is necessary to know about the endo- and exocytosis processes. Several experimental works indicate that endocytosis is progressively suppressed by increasing membrane tension (6,9,26,27). Indeed, the mechanical work needed to bud off a vesicle from a membrane grows as the tension increases (15). We take into account this tension-dependent endocytosis and assume, for simplicity, that the endocytosis rate decreases linearly with increasing membrane tension, up to a threshold tension σ_0 that fully prevents the formation of endocytic vesicles for tensions beyond this point. Namely, $k_D = k_D^0(1 - \sigma/\sigma_0)\Theta(1 - \sigma/\sigma_0)$, where $\Theta(\cdot)$ is the Heaviside step function. Although exocytic events can potentially depend on membrane tension, the major factor limiting exocytosis is whether the cell localizes exocytic vesicles to a particular region (1,2). Moreover, experimental data suggest that variations of exocytosis with membrane tension occur at timescales (1 min (5)) longer than typical timescales of exocytic processes (0.1–1 s (28)). Because of this separation in timescales, we assume here that exocytosis does not depend on membrane tension; variations at long timescales can be accounted for through adiabatic changes in the exocytosis profile. Given that many processes of cell shape changes involve polarized exocytosis, especially in walled cells (1,3,25), we assume a localized exocytosis profile $k_X(x) = (k_X^0/\sqrt{2\pi})\exp(-x^2/(2\lambda_X^2))$, characterized by magnitude k_X^0 and lengthscale λ_X.

Scaling length, time, and tension with λ_X ($\tilde{x} \equiv x/\lambda_X$), $(k_D^0)^{-1}$ ($\tilde{t} \equiv k_D^0\, t$) and σ_0 ($\tilde{\sigma} \equiv \sigma/\sigma_0$), respectively, the dynamics of the system is controlled

by four dimensionless parameters: the ratio of wall-expansion to exocytosis lengthscales, $\alpha \equiv \lambda_G/\lambda_X$; the ratio of a characteristic lengthscale, $\lambda_\sigma \equiv \sqrt{\sigma_0/((\xi+\xi_2)k_D^0)}$, associated with membrane tension variation to the exocytosis lengthscale, namely, $\beta \equiv \lambda_X/\lambda_\sigma$; the ratio of exo- to endocytosis membrane flow scales, $\kappa \equiv k_X^0\rho_X^0/(k_D^0\rho_0)$; and the ratio of wall-expansion rate to endocytosis rate, weighted by the relative strength of wall friction, $\gamma \equiv (g/k_D^0)(\xi_2/(\xi+\xi_2))$.

RESULTS

Solutions for the steady-state membrane tension and velocity profiles, $\sigma(x)$ and $v(x)$, respectively, can be analytically found for the localized exocytosis and wall-expansion profiles described above, imposing that no membrane flow or endocytosis exists at infinity ($v(x\to\pm\infty)\to 0$ and $k_D(x\to\pm\infty)\to 0$). In this case, the scaled membrane tension, $\tilde{\sigma}$, and velocity, $\tilde{v} \equiv v/(\lambda_X k_D^0)$, profiles read

$$\tilde{\sigma} = 1 - \frac{\beta\kappa}{4}\left(E_-^1(\tilde{x}) + E_+^1(\tilde{x})\right) + \frac{\beta\alpha\gamma}{4}\left(E_-^\alpha(\tilde{x}) + E_+^\alpha(\tilde{x})\right), \tag{4}$$

$$\tilde{v} = \frac{\kappa}{4}\left(E_-^1(\tilde{x}) - E_+^1(\tilde{x})\right) - \frac{\gamma\alpha}{4}\left(E_-^\alpha(\tilde{x}) - E_+^\alpha(\tilde{x})\right). \tag{5}$$

where $E_\pm^\alpha(\tilde{x}) \equiv e^{\frac{\beta^2\alpha^2}{2} \pm \beta\tilde{x}}\mathrm{erfc}((\beta\alpha^2 \pm \tilde{x})/(\alpha\sqrt{2}))$.

If the cell wall expansion is negligible ($\alpha\gamma \ll \kappa$) or, simply, there is no cell wall expansion ($\gamma = 0$), only two parameters, namely λ_X/λ_σ and $k_X^0\rho_X^0/(k_D^0\rho_0)$, determine the behavior of the system. When the friction of the membrane with the environment is small, membrane material flows away from the central region where exocytosis is large, because the excess membrane cannot be fully removed through endocytosis within this region (Fig. 2, *a* and *c*). In this case, both membrane tension and endocytosis vary over a large region of size $\lambda_\sigma \gg \lambda_X$ (Fig. 2, *b* and *d*), as indicated by the limiting expression $\tilde{\sigma} \simeq 1 - (\beta\kappa/2)e^{-x/\lambda_\sigma}$ for $x \gg \lambda_X$ (Fig. 2, *b* and *d*). On the other hand, if membrane flows are costly because of large friction with the environment, both membrane tension and endocytosis vary over a lengthscale similar to λ_X (Fig. 2, *b* and *d*). In this case, in-plane membrane flows become minimal and endocytosis removes the membrane excess in situ, as the endo- and exocytosis profiles become identical in this limit. The maximal membrane velocity and maximal endocytosis rate for these different regimes are shown in Fig. 2, *f* and *g*. In all scenarios, membrane tension is lowest when exocytosis is maximal and increases away from the exocytosis region toward its limiting value, σ_0 (Fig. 2 *b*), which ensures that no endocytosis exists in regions with no membrane flows or exocytosis. If a tension different from σ_0 were imposed at infinity, then solutions would only exist in the presence of additional global exocytosis, rather than just a localized source (see below). Finally, for every value of λ_X/λ_σ there exists a critical value of the ratio $k_X^0\rho_X^0/(k_D^0\rho_0)$ above which the membrane tension at the center (where exocytosis is maximal) becomes negative (Fig. 2 *b*), leading to an unstable situation (Fig. 2 *e*).

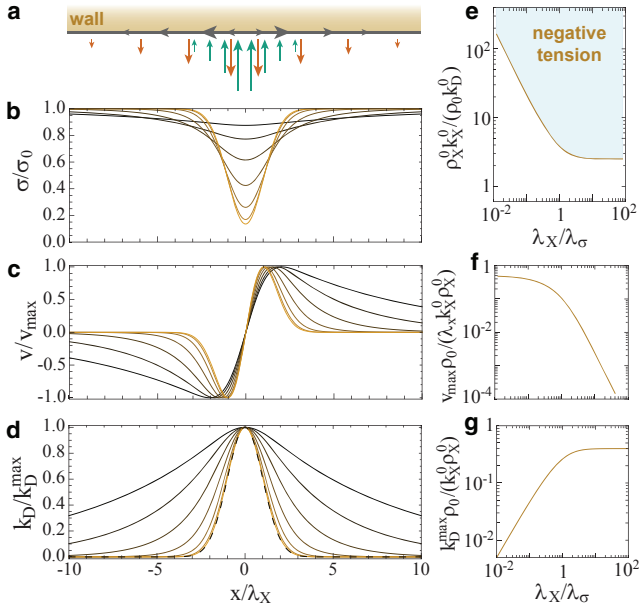

FIGURE 2 Membrane homeostasis in the absence of wall expansion. (*a*) Schematic representation of exocytosis, endocytosis, and the resulting membrane flows (*gray arrows* on membrane). The color scheme is the same as in Fig. 1. (*b–d*) Spatial dependence of normalized membrane tension, σ/σ_0 (*b*), velocity v/v_{max} (*c*), and endocytosis rate, k_D/k_D^{max} (*d*), at steady state. Solutions are shown for $\beta = \lambda_X/\lambda_\sigma = 1/8, 1/4, 1/2, 1, 2, 4, 8$ (*dark* to *bright*) and $\kappa = 2.2$. (*e*) Region of the parameter space where the negative tension values appear in the system. The bifurcation occurs for $\kappa \simeq 2/\beta$ for $\beta \ll 1$ and $\kappa = \sqrt{2\pi}$ for $\beta \gg 1$. (*f* and *g*) Dependence of the membrane maximum velocity, v_{max} (*f*), and maximum endocytosis rate, k_D^{max} (*g*), on β. For small β, v_{max} saturates to $\kappa/2$ and k_D^{max} grows as $\sim \beta/2$, whereas for large β, v_{max} drops as $\sim \kappa\beta^{-2}$ and k_D^{max} saturates to $1/(\sqrt{2\pi})$. The location where the membrane displays maximal velocity grows weakly as $\sim \sqrt{\ln\beta^{-2}}$ for $\beta \ll 1$ and is $\tilde{x} \approx 1$ for $\beta \gg 1$. To see this figure in color, go online.

In the presence of wall expansion, membrane homeostasis occurs only if the steady-state membrane dynamics can sustain the local areal expansion imposed by the wall. When the size of the exocytosis region is larger than the expansion region ($\lambda_X > \lambda_G$), the tension displays a local maximum at the center (Fig. 3 *b*), which results in an inward, converging membrane flow within a central region of size d_{in} (Fig. 3 *f*), and an outward membrane flow outside of this central region (Fig. 3, *a* and *c*). This is because the exocytosed membrane must go toward the center to balance the expansion occurring predominantly there. This membrane flow pattern, in which membrane flows converge toward the center due to the imposed surface expansion, provides a natural mechanism to concentrate transmembrane proteins in a specific region of the membrane, and could enhance or sustain cell polarization (18,19,29). In the opposite regime, when $\lambda_G > \lambda_X$, membrane tension is always minimal at the center and membrane flows away from the exocytic region (Fig. 3, *g* and *i*).

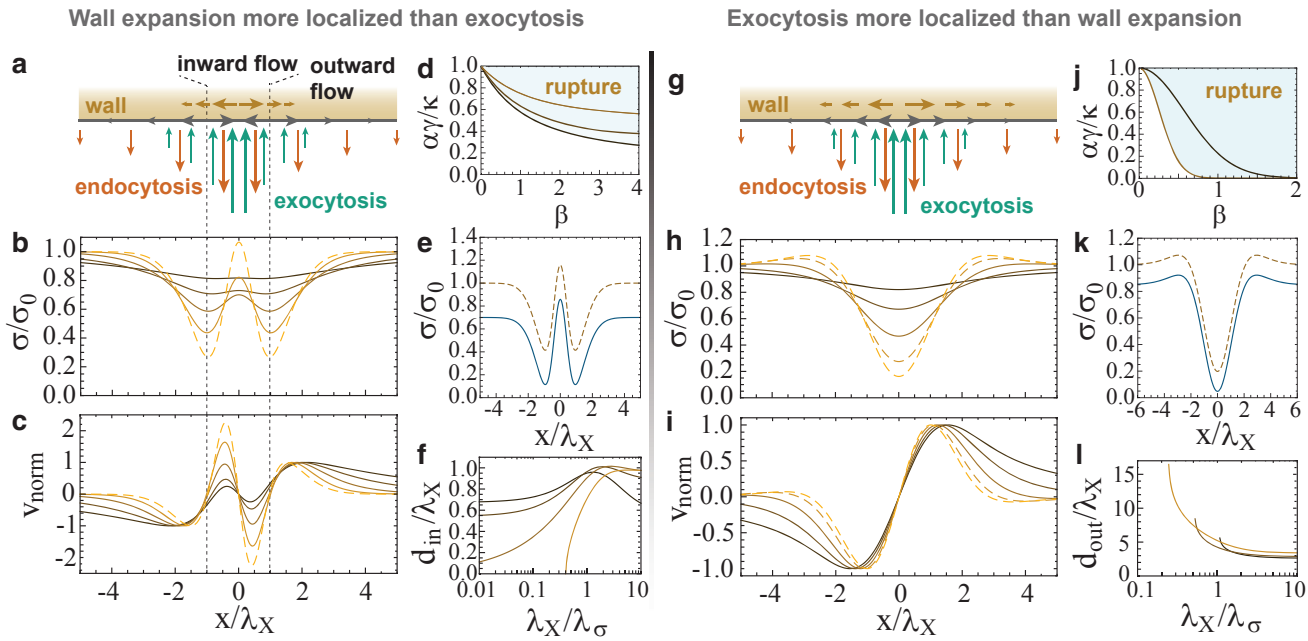

FIGURE 3 Membrane homeostasis in the presence of a locally expanding wall. The limiting regimes in which wall expansion is more localized ($\lambda_G < \lambda_X$) and less localized ($\lambda_G > \lambda_X$) than exocytosis are shown in (*a*)–(*f*) ($\lambda_G/\lambda_X = 0.4$) and (*g*)–(*l*)($\lambda_G/\lambda_X = 2$), respectively. (*a* and *g*) Schematic representations of exocytosis, endocytosis, wall expansion, and membrane flows in each regime. (*b*, *c*, *h*, and *i*) Tension, σ, and velocity, v (normalized to the second/first peak from the center in *c* and *h*), profiles for $\lambda_X/\lambda_\sigma = 1/4, 1/2, 1, 2, 4$ (*dark* to *bright*). Dashed curves indicate unstable solutions for which $\sigma > \sigma_0$. (*d* and *j*) Regions of the parameter space leading to membrane rupture (tension exceeding σ_0; *shaded areas*). The different curves define the transition from stable to unstable (membrane rupture) regions for $\lambda_G/\lambda_X = 1/8, 1/4, 1/2$ in (*d*) (*dark* to *bright*) and $\lambda_G/\lambda_X = 2, 4$ in (*j*) (*dark* to *bright*). (*e* and *k*) Adding a global exocytosis term stabilizes some of the unstable solutions by bringing the tension below σ_0. In all cases, the relative magnitude of expansion to exocytosis is $\alpha\gamma/\kappa = 0.5$, with $\kappa = 4$ for (*b*), (*c*), and (*e*) and $\kappa = 3$ for (*h*), (*i*), and (*k*). (*f* and *l*) Size of the central inward and outward flow regions, d_{in} (*f*) and d_{out} (*l*), respectively (see also Fig. 4), for $\lambda_G/\lambda_X = 0.2, 0.4, 0.5, 0.6$ in (*f*) (*dark* to *bright*) and $\lambda_G/\lambda_X = 1.5, 2.5, 5$ in (*l*) (*dark* to *bright*). $d_{in} \simeq \lambda_X$ for $\lambda_G \ll \lambda_X$, but can vanish for $\lambda_G \lesssim \lambda_X$, in which case, the inward flow disappears (*f*). Outward central flow forms only when a global exocytosis exists. $d_{out} \sim \lambda_X$ for $\lambda_\sigma \ll \lambda_X$, and $d_{out} \sim \lambda_\sigma$ for $\lambda_\sigma \gg \lambda_X$. d_{out} vanishes at a critical value of λ_X/λ_σ, for which the outward central flow disappears (*l*). To see this figure in color, go online.

Regardless of the type of membrane flows, there always exists a critical wall expansion rate, for which the existing exocytosis rate is not sufficient to balance the membrane expansion rate imposed by the wall, even when endocytosis is fully inhibited by tension ($\sigma = \sigma_0$), leading to membrane rupture (Fig. 3, *d* and *j*). The position for which tension exceeds σ_0 is at the center (Fig. 3 *b*) for $\lambda_G < \lambda_X$ and just out of the exocytosis region (Fig. 3 *h*) for $\lambda_G > \lambda_X$. Our results show that both strong enough wall expansion and large differences between the size of wall expansion and exocytosis regions can lead to rupture of the plasma membrane (Fig. 3, *d* and *j*). In the framework presented here, there exists a simple strategy to prevent this scenario. The presence of global exocytosis in addition to a localized exocytosis profile, lowers the tension by a constant factor (Fig. 3, *e* and *k*), which can be adjusted to keep the tension below σ_0 everywhere, thereby stabilizing the system and reducing the possibility of membrane rupture. Fig. 4 shows the required value of a global exocytosis rate, k_X^{global}, to stabilize the system as λ_G/λ_X is varied.

Beyond preventing membrane rupture, the addition of a global exocytosis leads to the appearance of new membrane flow patterns. When $\lambda_G > \lambda_X$, the system displays a central region of size d_{out} (Fig. 3 *l*) with outward, diverging membrane flow (away from the center), and inward membrane flow outside of this region (Fig. 4). This flow pattern is

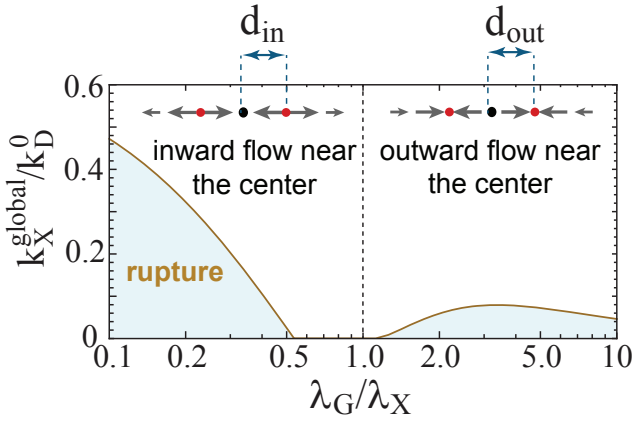

FIGURE 4 Membrane flow patterns for different values of λ_G/λ_X and global exocytosis rate k_X^{global}. Shaded areas correspond to membrane rupture due to tension exceeding σ_0. For a small expansion region compared to exocytosis ($\lambda_G < \lambda_X$), there is a stable inward flow near the center. In the opposite regime ($\lambda_G > \lambda_X$), the inward flow appears outside the exocytosis region. To see this figure in color, go online.

qualitatively different from that in the absence of global exocytosis, which is characterized only by outward flow for $\lambda_G > \lambda_X$ (Fig. 3 *g*). For $\lambda_G < \lambda_X$, the membrane flow pattern remains unchanged by global exocytosis (Fig. 3, *a* and *c*), but stabilizes this flow pattern for a larger region of the parameter space.

In addition to the potential membrane rupture for tension reaching σ_0, the membrane tension can also become negative. Considering only values of the parameters for which there is no membrane rupture, membrane tension becomes negative only when $\lambda_G \neq \lambda_X$, $\lambda_X \gg \lambda_\sigma$, and $k_X^0 \rho_X^0 \gg (k_D^0 \rho_0)$. This is qualitatively similar to the case of negligible cell wall expansion described above (Fig. 2 *e*), and it corresponds to situations with large relative friction forces and exocytosis rates, for which neither endocytosis nor membrane flows remove enough membrane to balance exocytosis.

DISCUSSION

We describe the dynamics of the cell's plasma membrane accounting for membrane recycling and membrane tension variations, in both the presence and absence of localized cell surface expansion. We obtain the steady-state membrane tension and endocytosis spatial profiles, as well as the in-plane membrane flows, that result from these dynamics. Overall, our results indicate that different spatial profiles of exo- and endocytosis necessarily generate in-plane membrane flows. Moreover, the interaction between the dynamics of the membrane and an adjacent, expanding mechanical structure (like the cell wall or cortex), leads to emerging membrane flow patterns. Finally, we obtain the conditions for membrane homeostasis in cells with expanding domains.

The predicted membrane flows correspond to membrane material moving under the force resulting from the membrane tension gradient. This situation resembles the Marangoni effect (30), where material moves at the interface of two fluids due to a gradient in the interfacial tension. In the case of the cell's plasma membrane, tension gradients are maintained out of equilibrium by spatial differences in exo- and endocytosis. In contrast to walled cells, for which spatial differences in the exo- and endocytosis profiles necessarily lead to in-plane membrane flows, animal cells can partially and transiently buffer local imbalances in exo- and endocytosis with membrane reservoirs, which may affect membrane flows.

In the presence of an expanding wall, membrane flow patterns emerge. Both regions of converging and diverging membrane flows can appear, depending on the relative lengthscales of the expansion and exocytosis regions. These flow patterns are predicted from simple spatial profiles of localized cell wall expansion and exocytosis, such as those observed in tip-growing walled cells. In animal cells, the interplay between cortical actin flows and membrane dynamics may lead to considerably more complex membrane flow patterns.

Beyond the dynamics of the membrane itself, these membrane flows can strongly influence the dynamics of membrane-localized proteins. Since diffusion of membrane-localized proteins tends to homogenize their density, the predicted membrane flow patterns could help explain the formation or stabilization of inhomogeneous distributions of membrane-localized proteins during cell polarization or other cellular processes involving cortical flows or cell wall expansion. Membrane flows could also potentially create cytoplasmic streaming in the vicinity of the plasma membrane and affect the dynamics of intracellular processes in this region.

Although they were obtained in 1D, our results capture the qualitative behavior of membrane dynamics in more realistic cell geometries. In the case of axisymmetric tip growth, which displays localized apical cell wall expansion and exocytosis, the changing surface geometry will affect the specific values for which certain membrane flows appear or the specific values at which membrane homeostasis is lost, but will not affect either the existence of flow patterns or the existence of a loss in membrane homeostasis. Therefore, although the results may change at a quantitative level for typically observed walled cell geometries, our qualitative results will be preserved. More generally, as cell shape changes are governed by the mechanics of the cell wall (membrane tension is much smaller than tension in the wall), the main change to the 1D dynamics presented here due to a cell's curved geometry will be curvature-induced amplifications or reductions of the membrane flows. For very complex and rapidly changing cell morphologies (e.g., animal cells), the interplay of local cell surface geometry and membrane flows can lead to new effects not captured in the 1D description presented here.

Our results show that membrane homeostasis can be sustained for a large range of parameters. However, we find that plasma membrane rupture can also occur. It is therefore important for the cell's viability to be in homeostatic states away from the instability threshold. Estimating all the dimensionless parameters that control the homeostatic (stable) states is challenging, because many kinetic or physicochemical parameters are unknown for cells of most organisms. In the case of fission yeast, some of the parameters can be estimated or bounded, allowing us to assess the homeostatic state of the membrane in this system. Measured values of the wall expansion and exocytosis lengthscales, as well as the expansion rate scale, g, in fission yeast ($\lambda_G \simeq 1.5\ \mu$m, $\lambda_X \simeq 2.0\ \mu$m, and $g \sim 10^{-2}\ s^{-1}$ (23,24)) indicate that the lengths of exocytosis and expansion are similar. Both exo- and endocytosis rates, k_X^0 and k_D^0, respectively, have been measured to be in the range $\sim 1 - 10\ s^{-1}$ (28). Assuming $\xi \sim \xi_2$, we estimate $\alpha\gamma/\kappa \sim 10^{-2}$. Although the estimation of the parameter β is more challenging, because no measurements exist for the tension σ_0, the membrane

tension, or the friction coefficients ξ and ξ_2 in fission yeast (as the presence of the cell wall makes the measurements very complex), the small value of $\alpha\gamma/\kappa \sim 10^{-2}$ puts the system well below the instability threshold for membrane rupture (Fig. 3 *d*). Finally, our predictions indicate that increasing the cell wall expansion rate, either by modifying the cell wall mechanics or increasing the turgor pressure, as well as varying the exocytosis profile, can all induce rupture of the plasma membrane.

More generally, the interplay between the dynamics of the plasma membrane and the expansion of the cell wall in walled cells or the cell cortex in animal cells, can lead to complex plasma membrane flows, potentially affecting a wide range of cellular processes.

AUTHOR CONTRIBUTIONS

O.C. defined and supervised the project. P.R. performed theoretical analysis. O.C. and P.R. wrote the article.

ACKNOWLEDGMENTS

We thank the National Institute of General Medical Sciences of the National Institutes of Health (award number R01GM113241) for financial support.

REFERENCES

1. Harold, F. M. 2005. Molecules into cells: specifying spatial architecture. *Microbiol. Mol. Biol. Rev.* 69:544–564.
2. Lecuit, T., and F. Pilot. 2003. Developmental control of cell morphogenesis: a focus on membrane growth. *Nat. Cell Biol.* 5:103–108.
3. Fowler, J. E., and R. S. Quatrano. 1997. Plant cell morphogenesis: plasma membrane interactions with the cytoskeleton and cell wall. *Annu. Rev. Cell Dev. Biol.* 13:697–743.
4. Heisenberg, C.-P., and Y. Bellaïche. 2013. Forces in tissue morphogenesis and patterning. *Cell.* 153:948–962.
5. Gauthier, N. C., M. A. Fardin, …, M. P. Sheetz. 2011. Temporary increase in plasma membrane tension coordinates the activation of exocytosis and contraction during cell spreading. *Proc. Natl. Acad. Sci. USA.* 108:14467–14472.
6. Gauthier, N. C., T. A. Masters, and M. P. Sheetz. 2012. Mechanical feedback between membrane tension and dynamics. *Trends Cell Biol.* 22:527–535.
7. Morris, C. E., and U. Homann. 2001. Cell surface area regulation and membrane tension. *J. Membr. Biol.* 179:79–102.
8. Diz-Muñoz, A., D. A. Fletcher, and O. D. Weiner. 2013. Use the force: membrane tension as an organizer of cell shape and motility. *Trends Cell Biol.* 23:47–53.
9. Sheetz, M. P. 2001. Cell control by membrane-cytoskeleton adhesion. *Nat. Rev. Mol. Cell Biol.* 2:392–396.
10. Sinha, B., D. Köster, …, P. Nassoy. 2011. Cells respond to mechanical stress by rapid disassembly of caveolae. *Cell.* 144:402–413.
11. Norman, L. L., J. Brugués, …, H. Aranda-Espinoza. 2010. Cell blebbing and membrane area homeostasis in spreading and retracting cells. *Biophys. J.* 99:1726–1733.
12. Charras, G., and E. Paluch. 2008. Blebs lead the way: how to migrate without lamellipodia. *Nat. Rev. Mol. Cell Biol.* 9:730–736.
13. Figard, L., M. Wang, …, A. M. Sokac. 2016. Membrane supply and demand regulates F-actin in a cell surface reservoir. *Dev. Cell.* 37: 267–278.
14. Groulx, N., F. Boudreault, …, R. Grygorczyk. 2006. Membrane reserves and hypotonic cell swelling. *J. Membr. Biol.* 214:43–56.
15. Sens, P., and M. S. Turner. 2006. Budded membrane microdomains as tension regulators. *Phys. Rev. E Stat. Nonlin. Soft Matter Phys.* 73:031918.
16. Sens, P. 2004. Dynamics of nonequilibrium membrane bud formation. *Phys. Rev. Lett.* 93:108103.
17. Firat-Karalar, E. N., and M. D. Welch. 2011. New mechanisms and functions of actin nucleation. *Curr. Opin. Cell Biol.* 23:4–13.
18. Cole, R. A., and J. E. Fowler. 2006. Polarized growth: maintaining focus on the tip. *Curr. Opin. Plant Biol.* 9:579–588.
19. Goehring, N. W., and S. W. Grill. 2013. Cell polarity: mechanochemical patterning. *Trends Cell Biol.* 23:72–80.
20. Asnacios, A., and O. Hamant. 2012. The mechanics behind cell polarity. *Trends Cell Biol.* 22:584–591.
21. Tabdanov, E., N. Borghi, …, J.-P. Thiéry. 2009. Role of E-cadherin in membrane-cortex interaction probed by nanotube extrusion. *Biophys. J.* 96:2457–2465.
22. Brochard-Wyart, F., N. Borghi, …, P. Nassoy. 2006. Hydrodynamic narrowing of tubes extruded from cells. *Proc. Natl. Acad. Sci. USA.* 103:7660–7663.
23. Abenza, J. F., E. Couturier, …, R. E. Carazo Salas. 2015. Wall mechanics and exocytosis define the shape of growth domains in fission yeast. *Nat. Commun.* 6:8400.
24. Dumais, J., S. R. Long, and S. L. Shaw. 2004. The mechanics of surface expansion anisotropy in *Medicago truncatula* root hairs. *Plant Physiol.* 136:3266–3275.
25. Campàs, O., and L. Mahadevan. 2009. Shape and dynamics of tip-growing cells. *Curr. Biol.* 19:2102–2107.
26. Rauch, C., and E. Farge. 2000. Endocytosis switch controlled by transmembrane osmotic pressure and phospholipid number asymmetry. *Biophys. J.* 78:3036–3047.
27. Dai, J., and M. P. Sheetz. 1995. Regulation of endocytosis, exocytosis, and shape by membrane tension. *Cold Spring Harb. Symp. Quant. Biol.* 60:567–571.
28. Carrillo, L., B. Cucu, …, A. Bertl. 2015. High-resolution membrane capacitance measurements for studying endocytosis and exocytosis in yeast. *Traffic.* 16:760–772.
29. Mellman, I., and W. J. Nelson. 2008. Coordinated protein sorting, targeting and distribution in polarized cells. *Nat. Rev. Mol. Cell Biol.* 9:833–845.
30. Scriven, L. E., and C. V. Sternling. 1960. The Marangoni effects. *Nature.* 187:186–188.